Available online at www.sciencedirect.com
ScienceDirect
International Journal of Rock Mechanics & Mining Sciences 45 (2008) 1500–1507
International Journal of Rock Mechanics and Mining Sciences
www.elsevier.com/locate/ijrmms

Technical Note

Normal stiffness of fractures in granitic rock: A compilation of laboratory and in-situ experiments

C. Zangerl[a,b,*], K.F. Evans[a], E. Eberhardt[a,c], S. Loew[a]

[a]*Engineering Geology, Swiss Federal Institute of Technology (ETH Zurich), Zurich, Switzerland*
[b]*alpS GmbH, Centre for Natural Hazard Management, Grabenweg 3, A-6020 Innsbruck, Austria*
[c]*Geological Engineering/Earth and Ocean Sciences, University of British Columbia, Vancouver, Canada*

Received 13 February 2008; accepted 14 February 2008
Available online 1 April 2008

1. Introduction

Fractures and the networks they form have a major impact on the mechanical, thermal and hydraulic behaviour of a rock mass. For this reason, practically all geotechnical engineering projects conducted in fractured rock require quantitative descriptions of the properties of the fractures. A case in point is the project that motivated this study: the simulation of the surface subsidence resulting from the drawdown in pore-pressure about a deep tunnel in crystalline rock due to drainage into the tunnel [1,2]. Hydro-mechanically coupled discontinuum models of the medium required properties to be assigned, amongst which was the stress-dependent normal stiffness characteristics. Since there were no estimates of such for the fractures within the rock mass in question, a survey of published studies of normal stiffness was undertaken to guide the model parameterisation. Most studies measured fracture closure as a function of a change in applied effective normal stress. In laboratory experiments, the change was usually cyclical. A key problem in rendering such diverse data to be collectively interpretable is posed by the fact that the normal stiffness of fractures, k_n, is strongly stress dependent, particularly at low effective normal stress levels (Fig. 1). This means that the closure-normal stress curves must be approximated by some function that fits the curves, preferably with as few free parameters as possible. Based on laboratory tests, Goodman [3] proposed an empirical hyperbolic fracture closure law, which has two free parameters. Bandis et al. [4] found this to be appropriate for mated fractures. However, Bandis et al. [4] concluded that the closure behaviour of non-mated fractures was better described by a semi-logarithmic closure law wherein closure varies as the logarithm of normal stress. Zhao and Brown [5] and Evans et al. [6] applied the semi-logarithmic closure law to both shear and tensile fractures. Walsh and Grosenbough [7] have shown that the semi-logarithmic closure law arises quite naturally from the closure of surfaces whose topography is characterised by a distribution of summit asperity heights that is exponential. The semi-logarithmic closure law has advantage over other stiffness laws in that it has only one free parameter, which we will refer to as the "stiffness characteristic" [6]. Thus, the stress-dependent normal stiffness characteristics of a fracture are completely determined by specifying this parameter. Moreover, its value can be derived from a single closure measurement performed over a small stress range, as is often the case with in-situ tests. In view of the above, the semi-logarithmic closure law was used in the study.

The primary purpose of this technical note is to list the values of the stiffness characteristic obtained from the analysis of published laboratory and in-situ test, and examine the implications for assigning stiffness characteristics to fractures in simulation studies. It is not the intention to critically compare the semi-logarithmic closure relation with other relations that have been proposed [3,4]. These generally have more free parameters and thus might be expected to fit the data more comprehensively. The aim is to render a large body of data within a framework of

DOI of original article: 10.1016/j.ijrmms.2008.02.002
*Corresponding author at: alpS-Centre for Natural Hazard Management-GmbH, Grabenweg 3, A-6020 Innsbruck, Austria.
Tel.: +43 512 392929 14; fax: +43 512 392929 39.
E-mail address: zangerl@alps-gmbh.com (C. Zangerl).

1365-1609/$ - see front matter
doi:10.1016/j.ijrmms.2008.02.001

stiffness characterisation that permits collective analysis, so that the range of behaviour can be simply assessed to yield results of engineering utility.

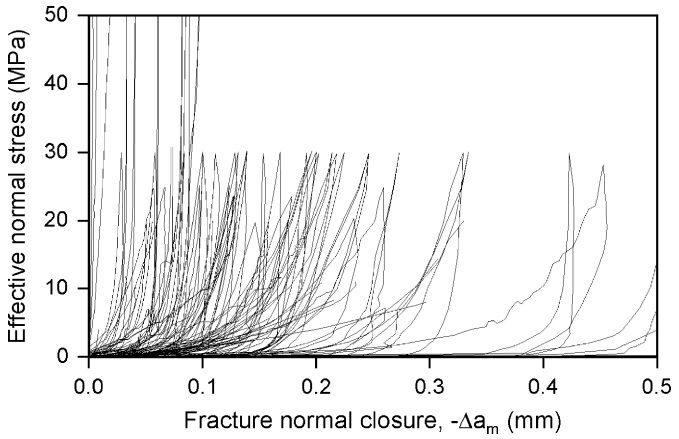

Fig. 1. Laboratory and in-situ experiments showing highly non-linear normal closure behaviour, and hysteresis which is particularly pronounced on the first loading cycle.

2. Semi-logarithmic closure law

Fracture normal stiffness, k_n, is defined as the instantaneous slope of the effective normal stress versus fracture aperture change curve, and has dimensions of Pascals per metres. For the semi-logarithmic closure law, the predicted change in mechanical aperture, Δa_m, resulting from a change in effective normal stress from an arbitrary reference value σ_n^{ref} to a value σ'_n, is given by

$$-\Delta a_m = \frac{1}{dk_n/d\sigma'_n}\ln(\sigma'_n/\sigma_n^{ref}) \quad (1)$$

where $dk_n/d\sigma'_n$ is a constant that will be referred to as the "stiffness characteristic" [6]. It can be shown that for the semi-logarithmic closure law, the curve of normal stiffness versus effective normal stress is linear and passes through the origin (i.e. zero stiffness at zero normal stress), giving:

$$k_n = \left(\frac{dk_n}{d\sigma'_n}\right)\sigma'_n \quad (2)$$

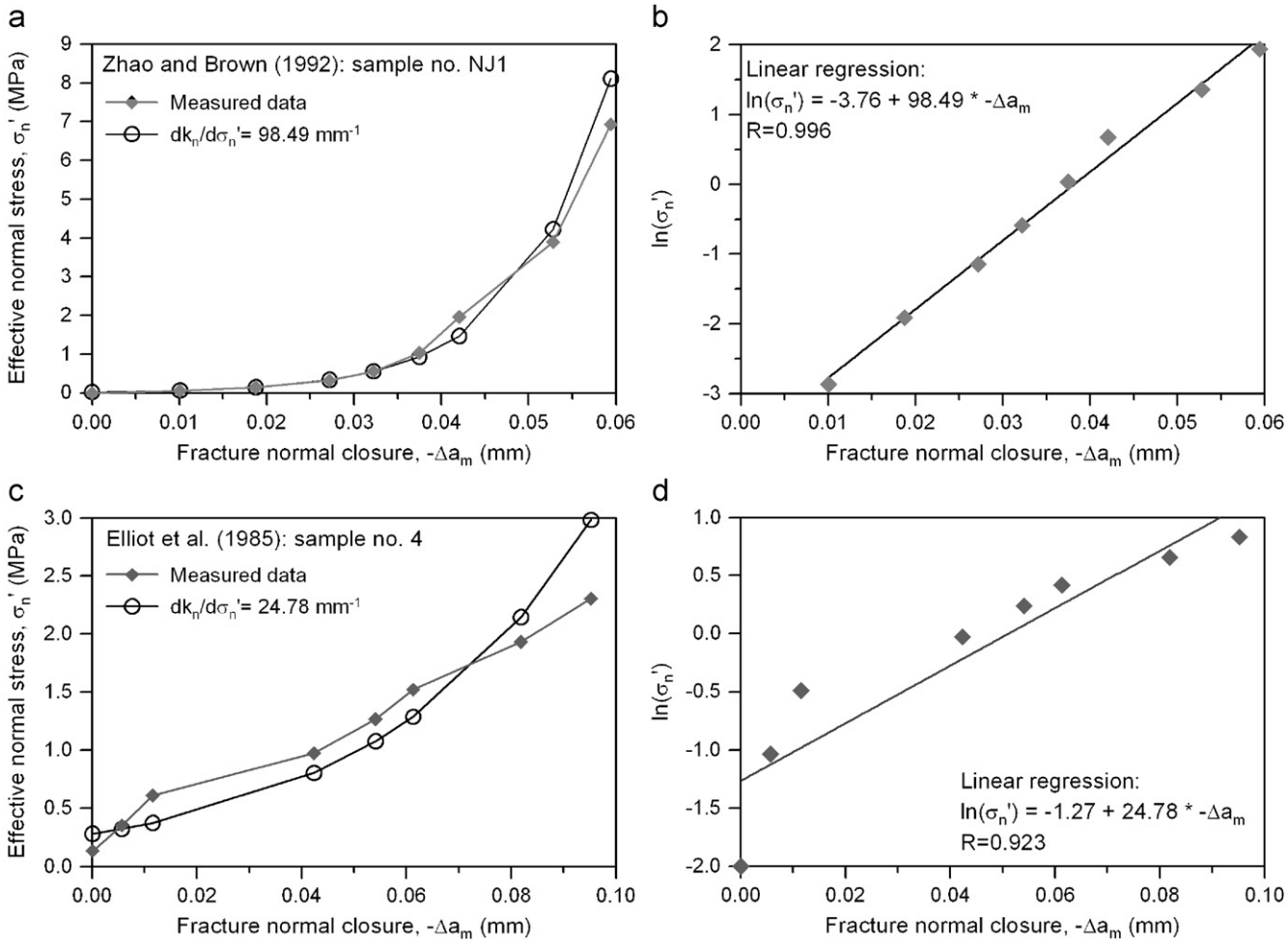

Fig. 2. Fitting of the logarithmic closure law to measured data sets: (a) comparison between measured values from Zhao and Brown [5] and fitted values based on a stiffness characteristic of $dk_n/d\sigma'_n = 98.49\,mm^{-1}$, (b) linear regression analysis of Zhao and Brown's data showing a good fit characterised by a high value of $R = 0.996$ [5], (c) comparison between measured values from Elliot et al. [15] and fitted values based on a stiffness characteristic of $dk_n/d\sigma'_n = 24.78\,mm^{-1}$, and (d) linear regression analysis showing the poor fit of Elliot et al.'s data characterised by a low value of $R = 0.923$ [15].

Table 1
Survey of published laboratory and in-situ joint normal closure experiments on meso-scale fractures in granitic rock (as defined using a semi-logarithmic closure law, where $dk_n/d\sigma'_n$ = stiffness characteristic, σ'_n = effective normal stress, and R = coefficient of determination)

Rock type, fracture type	Fracture dimensions	Sample # (loading cycle)	$\sigma'_{n\,min}$ (MPa)	$\sigma'_{n\,max}$ (MPa)	Stiffness characteristic		Ref.
					$dk_n/d\sigma'_n$ (mm^{-1})	R	
Laboratory experiments							
Charcoal granite, artificial fracture	11.2 × 24.8 cm	1 (1)	0.033	7.0	21	0.99	[14]
Carnmenellis granite, clean natural fracture	5.1 × 10.2 cm	2 (1)	0.107	4.0	28	0.98	[15]
		3 (1)	0.363	6.0	39	0.96	
		4 (1)	0.282	2.0	25	0.92	
		5 (1)	0.095	4.0	61	0.99	
Charcoal black granite, clean natural fracture	10 cm diameter	1 (1)	0.085	30.0	28	0.99	[16]
		1 (2)	0.282	30.0	81	0.99	
		1 (3)	0.407	30.0	149	0.99	
	15 cm diameter	2 (1)	0.004	30.0	28	0.99	
		2 (2)	0.023	30.0	75	0.97	
		2 (3)	0.038	30.0	82	1.00	
	19.3 cm	3 (1)	0.257	30.0	24	1.00	
	diameter	3 (2)	0.029	30.0	53	0.98	
		3 (3)	0.027	30.0	56	0.98	
	29.4 cm	5 (1)	0.076	24.0	35	0.95	
	diameter	5 (2)	0.093	24.0	46	0.98	
		5 (3)	0.056	24.0	51	0.98	
Granodiorite, natural fracture coated with iron oxide and pyrite	28.2 × 25.4 cm	1 (1)	0.017	20.0	22	0.99	[17]
		1 (2)	0.000	17.0	26	0.99	
		1 (3)	0.002	14.0	27	0.94	
		1 (4)	0.000	16.0	18	0.96	
Pinawa granite, natural fracture	15.9 cm	H1 (1)	0.380	30.0	57	0.98	[18]
	diameter	H1 (3)	0.191	30.0	57	0.93	
Stripa granite, natural fracture	15.4 cm	STR2 (1)	0.011	20.0	6	1.00	[18]
	diameter	STR2 (2)	0.051	20.0	28	0.94	
		STR2 (3)	0.036	20.0	43	0.99	
Granite, natural fracture	12 cm diameter	4–1 (–)	0.027	80.0	115	0.91	[19]
		4–2 (–)	0.028	80.0	84	0.97	
Stripa granite (Quartz monzonite), natural fracture	5.2 cm	E35 (1)	4.074	85.0	130	0.95	[20]
	diameter	E30 (2)	2.399	85.0	431	0.99	
		E32 (3)	2.630	85.0	720	0.97	
Charcoal black granite, natural fracture	91.4 cm diameter	1 (4)	0.009	20.0	113	0.90	[21]
Stripa granite, natural fracture coated with chlorite	20 cm diameter	1 (1)	0.148	25.0	20	0.99	[9]
		1 (2)	1.413	25.0	45	0.99	
		1 (3)	1.778	25.0	48	0.99	
		2 (1)	0.048	27.0	14	0.99	
		2 (2)	0.081	27.0	66	0.99	
Granite, artificial tension fracture	15 cm diameter	1 (1)	0.002	20.0	79	0.98	[22]
Carnmenellis granite, natural shear fractures and artificial tension fractures	5.1 × 10.2 cm	EF1 (1)	0.117	8.0	60	1.00	[5]
		EF3 (1)	0.316	2.5	56	0.99	
		NJ1 (1)	0.023	7.0	98	1.00	
		NJ6 (1)	0.141	3.8	26	0.99	
Westerly granite (artificial fracture)	15 × 14 cm	2 (–)	0.025	160.0	78	0.97	[23]
Red granite, artificial fracture previously sheared	731 cm^2	1 (2,3)	0.148	2.7	27	0.99	[24]
		12 (1)	0.115	2.7	26	0.96	
		13 (1)	0.234	5.5	21	0.98	
		14 (1)	0.263	8.2	17	0.98	
		15 (1)	0.191	10.9	18	0.97	
		60 (1)	0.347	8.2	12	0.96	

Table 1 (*continued*)

Rock type, fracture type	Fracture dimensions	Sample # (loading cycle)	$\sigma'_{n\,min}$ (MPa)	$\sigma'_{n\,max}$ (MPa)	Stiffness characteristic		Ref.
					$dk_n/d\sigma'_n$ (mm^{-1})	R	
		63 (1)	0.126	5.5	21	1.00	
		66 (1)	0.107	2.7	28	0.99	
		69 (1)	0.138	10.9	22	1.00	
Grey granite, artificial tension fracture	1009 cm^2	3 (1)	0.234	4.0	18	0.96	[24]
		4 (1)	0.031	2.0	108	0.98	
		5 (1)	0.091	5.9	54	0.96	
		23 (1)	0.302	2.0	88	0.89	
		24 (1)	0.055	4.0	52	0.98	
		25 (1)	0.069	5.9	28	1.00	
Dolerite, fresh natural fracture	4–6 × 8–10 cm	1 (1)	0.117	50.0	68	0.99	[4]
		1 (2)	0.257	50.0	123	0.99	
		1 (3)	0.302	50.0	141	0.99	
Granite, artificial tension fracture	Not reported	1 (–)	0.071	25.0	56	0.98	[25]
Granitic gneiss, artificial and natural fractures	15 × 30 cm	9 (1)	0.000	30.0	48	0.98	[26]
		9 (2)	0.001	30.0	65	0.96	
		9 (3)	0.000	30.0	113	0.99	
		10 (1)	0.000	30.0	29	0.97	
		10 (2)	0.000	30.0	57	0.99	
		10 (3)	0.001	30.0	98	0.96	
		33 (1)	0.005	30.0	25	0.97	
		33 (2)	0.000	30.0	57	0.94	
		33 (3)	0.002	30.0	51	0.96	
		34 (1)	0.000	30.0	52	1.00	
		34 (2)	0.003	30.0	40	0.98	
		34 (3)	0.002	30.0	41	0.97	
		40 (1)	0.126	30.0	27	1.00	
		40 (2)	0.001	30.0	82	0.97	
		41 (1)	0.044	30.0	32	0.96	
		41 (3)	0.066	30.0	34	0.98	
		42 (1)	0.058	30.0	36	0.99	
		42 (2)	0.011	30.0	63	0.99	
		42 (3)	0.004	30.0	65	0.99	
Granite, natural fractures	5.1 × 10.2 cm	A01 (6)	0.056	12.0	151	0.99	[27]
		A03 (6)	0.100	4.0	48	0.99	
		A07 (6)	0.089	10.0	114	0.99	
		A08 (6)	0.076	4.0	462	1.00	
Kikuma granodiorite, artificial tension and clean natural fractures	5 × 10 cm	Natural (1)	0.372	20.0	23	0.99	[28]
		Natural (2)	0.398	20.0	68	0.97	
		Natural (3)	0.417	20.0	64	0.98	
		Tension (1)	0.724	20.0	17	0.99	
		Tension (2)	1.259	20.0	21	0.99	
		Tension (3)	1.175	20.0	21	0.98	
In-situ experiments							
Stripa granite (in-situ), natural fracture, coated with chlorite	100 × 140 cm	3(1)	0.204	10.0	44	0.99	[9]
Falkenberg granite (in situ), artificial fracture		HB4a (1)	0.141	1.9	4	0.96	[11]
		SB5 (1)	0.138	1.9	3	0.93	
Sherman granite (in situ), fresh natural fracture	280 × 260 cm	D5 (1)	0.087	4.0	89	0.96	[8]
		D4 (1)	0.083	4.0	24	0.99	
		D6 (1)	0.072	4.0	19	0.99	
	2 fractures	D2 (1)	0.107	4.0	5	0.93	
		D3 (11)	0.204	6.0	12	0.99	[7]
Granite (in situ), natural fracture		1 (–)	–	1.5	<13	–	[12]
Granite (in situ), natural fractures		L81[a]	–	1.4	21	–	[13]

Table 1 (*continued*)

Rock type, fracture type	Fracture dimensions	Sample # (loading cycle)	$\sigma'_{n\,min}$ (MPa)	$\sigma'_{n\,max}$ (MPa)	Stiffness characteristic		Ref.
					$dk_n/d\sigma'_n$ (mm^{-1})	R	
Clean and coated with soft minerals		L131[a]	–	2.2	227	–	
		L257[a]	–	3.4	37	–	
		L283[a]	–	3.2	156	–	
		L357[a]	–	5.9	169	–	
		L417[a]	–	7.3	151	–	
		Ä266[a]	–	4.8	208	–	
		Ä267[a]	–	4.3	233	–	
		Ä315[a]	–	4.6	217	–	
		Ä316[a]	–	3.9	19	–	
		Ä336[a]	–	4.1	27	–	
		Ä337[a]	–	4.1	244	–	
		Ä338[a]	–	4.1	244	–	
Lac du bonnet granite (in situ),		OC1	–	8.6	41	–	[10]
Natural tension fractures		OC1	–	8.6	74	–	

[a]In-situ values back-calculated through numerical modelling of well tests.

The constant, $dk_n/d\sigma'_n$, thus completely describes the normal stiffness behaviour of the fracture. It follows that the normal stiffness of the fracture, k_n, at any effective normal stress level, σ'_n, can be obtained by multiplying the value of the stiffness characteristic by the effective normal stress (see Eq. (2)).

3. Estimation of the stiffness characteristic from published laboratory and in-situ experiments

A large number of "closure versus normal stress" curves from laboratory and in-situ tests published in the literature were fitted to Eq. (1) to estimate the implied stiffness characteristic values (Fig. 2). Digital data were not available in most cases and hence the curves were scanned and digitised. The data were then plotted as the natural logarithm of normal stress $\ln(\sigma'_n)$ versus normal closure $-\Delta a_m$. A linear regression was then performed to fit the curve to the linear relationship:

$$\ln(\sigma'_n) = A(-\Delta a_m) + B \quad (3)$$

Comparison of this relation to Eq. (1) shows that A is the stiffness characteristic and B is the natural logarithm of the reference normal stress σ_n^{ref}. The latter is the effective normal stress level at the start of the test when $\Delta a_m = 0$, and was generally small (i.e. <4 MPa, see $\sigma'_{n\,min}$ in Table 1). The linear regression analysis yielded estimates for A, B and also the regression coefficient R, which represents the root mean square deviation of the data from the best-fitting straight line. R is a measure of the degree to which the data conform to a semi-log closure law.

The data we included in the study mostly derive from tests on predominantly unfilled, naturally or artificially generated fractures in granitic rocks. A few fractures with surfaces coated by chlorite or iron oxides were also included but no tests on fractures that contained fault gouge and breccia were included. Most tests, whether they were laboratory or in-situ, used several loading cycles. In situ experiments featured in the study estimated the closure versus stress curves from either flatjack tests [8,9], or borehole pressure tests that used specially developed packer systems to measure fracture aperture changes (PAC-ex-system [10,11]), or computed the aperture change from surface deformation [12], or derived the normal stiffness from back-calculation of hydraulic tests in fractures [13]. The in-situ tests were all conducted at effective normal stress levels less than 10 MPa, whereas the range for laboratory experiments extended up to 160 MPa (Table 1).

4. Results

The results from 115 normal closure experiments are listed in Table 1 [4,5,7–28]. A histogram showing the value of the regression coefficient is shown in Fig. 3. The regression coefficient R is the root mean square deviation of the best-fitting semi-log closure curve to the data curve. From visual inspection, it was concluded that values of R greater than 0.93 represent satisfactory fits to the data. Thus, the majority of the closure-normal stress curves conformed adequately to a semi-logarithmic closure law described by the single parameter, the stiffness characteristic. Fig. 3 also shows the histograms of the regression coefficients for first cycle curves and those from later cycles. No systematic improvement in the quality of fit is seen for later cycle tests.

The range of values of the stiffness characteristic from all tests is shown in the histogram of Fig. 4. The values span

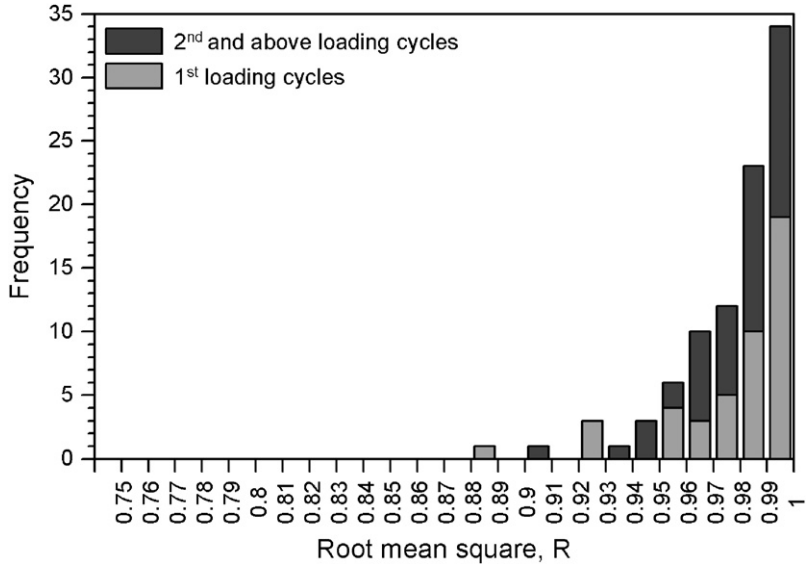

Fig. 3. Histogram of root mean square values, R, grouped into first and second and later loading cycles.

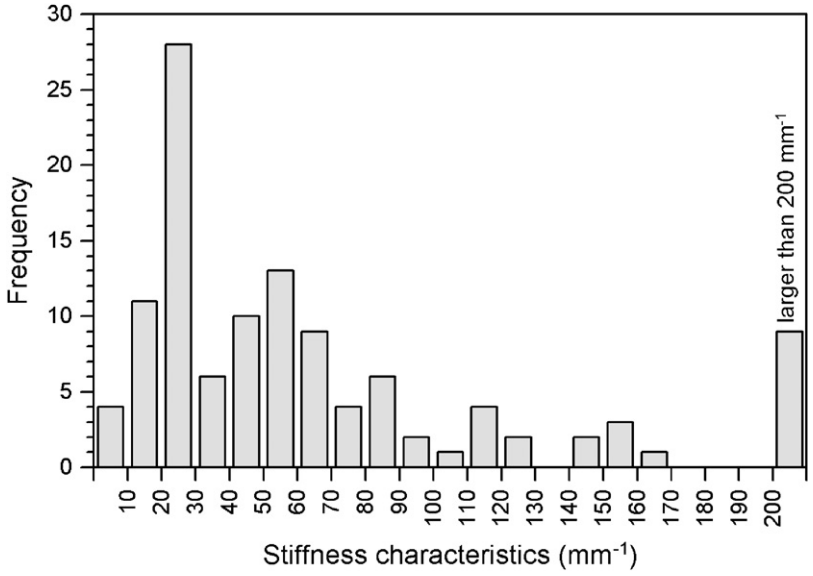

Fig. 4. Histogram of stiffness characteristic values (all data).

an enormous range: from 720 mm^{-1} for well-mated fractures in laboratory tests to 3 mm^{-1} for an in-situ test on an induced or reactivated hydrofracture isolated in a borehole [11]. The form of the distribution is heavily influenced by the data that happened to be available for inclusion in the study. Nevertheless, it can be concluded that fractures with stiffness characteristic values in the range 10–70 mm^{-1} are relatively common. A low value of stiffness characteristic implies a relatively compliant fracture. For example, a fracture that has the lowest value identified in the study of 3 mm^{-1} and supports an effective normal stress of 1 MPa would from Eq. (2) have a normal stiffness of 3 MPa/mm. It was also observed that the stiffness characteristic values for the first loading cycle are generally lower than for values obtained from tests under higher loading cycles (Fig. 5). The highest stiffness characteristic value was obtained from laboratory tests of a well-mated 21 cm^2 fracture in Stripa granite [20]. All high values were obtained from laboratory tests on small sample sizes (Fig. 6). However, there is only weak evidence of a systematic scale effect for fracture cross-sectional areas of more than 100 cm^2.

5. Conclusion

Results from linear regression analysis of 115 different laboratory and in-situ normal closure experiments in granitic rock showed a very large range of stiffness characteristic values, even for well-defined laboratory tests within the same rock type. This was not unexpected

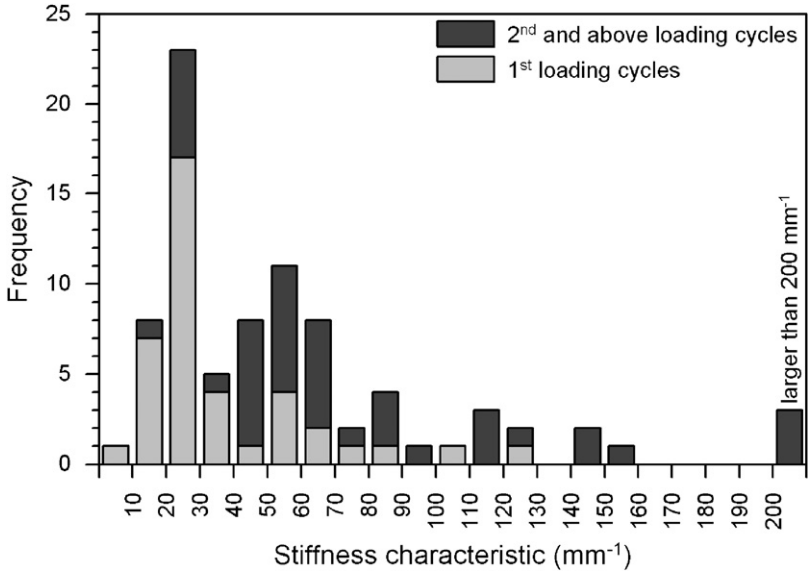

Fig. 5. Histogram of stiffness characteristic values, grouped into first and second and later loading cycle values.

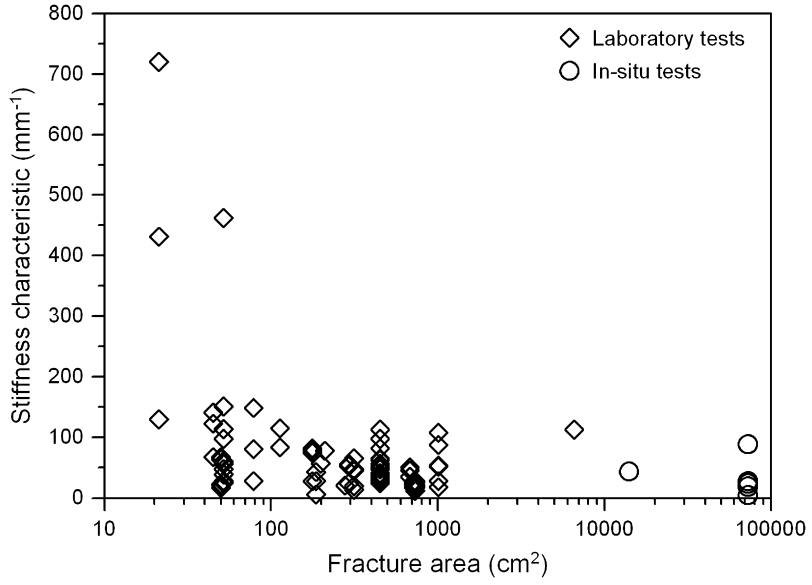

Fig. 6. Relationship between fracture area in cm^2 and stiffness characteristics in mm^{-1} (circles = in-situ experiments, diamonds = laboratory experiments).

because fracture normal stiffness is highly affected by several, extreme complex interacting factors (i.e. fracture surface geometry, asperity deformability, fracture interlocking, testing conditions, etc.) which are discussed in detail in [3–8,29]. Given that under in-situ conditions most of these factors are difficult or impossible to determine, this study is intended to provide some ranges of stiffness characteristic values for practitioners involved in geotechnical projects in fractured rock masses where site-specific normal stiffness tests are not available. It was found that the semi-logarithmic normal closure law provided a satisfactory description of the closure behaviour of these tests and therefore only the single parameter of stiffness characteristic is needed to estimate the normal stiffness at arbitrary normal stress levels.

References

[1] Zangerl C, Evans KF, Eberhardt E, Loew S. Consolidation settlements above deep tunnels in fractured crystalline rock: part 1—investigation above the Gotthard highway tunnel. Int J Rock Mech Min Sci 2008, doi:10.1016/j.ijrmms.2008.02.002.

[2] Zangerl C, Eberhardt E, Evans KF, Loew S. Consolidation settlements above deep tunnels in fractured crystalline rock: part 2—numerical analysis of the Gotthard highway tunnel case study. Int J Rock Mech Min Sci 2008, doi:10.1016/j.ijrmms.2008.02.005.

[3] Goodman RE, Taylor R, Brekke T. A model for the mechanics of jointed rock. J Soil Mech Found Div ASCE 1968;94(SM3):367–659.
[4] Bandis SC, Lumsden AC, Barton NR. Fundamentals of rock joint deformation. Int J Rock Mech Min Sci 1983;20(6):249–68.
[5] Zhao J, Brown ET. Hydro-thermo-mechanical properties of joints in the Carnmenellis granite. Q J Eng Geol 1992;25:279–90.
[6] Evans KF, Kohl T, Rybach L, Hopkirk RJ. The effects of fracture normal compliance on the long term circulation behaviour of a hot dry rock reservoir: a parameter study using the new fully-coupled code fracture. Trans Geotherm Resourc Counc 1992;16:449–56.
[7] Walsh JB, Grosenbaugh MA. A new model for analyzing the effect of fractures on compressibility. J Geophys Res 1979;84(B7):3532–6.
[8] Pratt HR, Swolfs HS, Brace WF, Black AD, Handin JW. Elastic and transport properties of an in-situ jointed granite. Int J Rock Mech Min Sci 1977;14:34–45.
[9] Makurat A, Barton N, Tunbridge L, Vik G. The measurement of the mechanical and hydraulic properties of rock joints at different scales in the Stripa project. In: Barton N, Stephansson O, editors. Proceedings of international conference on rock joints, Loen, Norway. Rotterdam: Balkema; 1990. p. 541–8.
[10] Martin CD, Davison CC, Kozak ET. Characterizing normal stiffness and hydraulic conductivity of a major shear zone in granite. In: Barton N, Stephansson O, editors. Proceeding of the international conference on rock joints, Loen, Norway. Rotterdam: Balkema; 1990. p. 549–56.
[11] Jung R. Hydraulic in situ investigations of an artificial fracture in the Falkenberg Granite. Int J Rock Mech Min Sci 1989;26(3/4):301–8.
[12] Evans K, Wyatt F. Water table effects on the measurements of earth strain. Tectonophysics 1984;108:323–37.
[13] Rutqvist J, Noorishad J, Tsang C-F, Stephansson O. Determination of fracture storativity in hard rocks using high-pressure injection testing. Water Resourc Res 1998;34(10):2551–60.
[14] Detournay E. Hydraulic conductivity of closed rock fracture: An experimental and analytical study. In: Proceeding of the 13th can rock mechanical symposium underground rock engineering, Toronto, 1980. p. 168–73.
[15] Elliott GM, Brown ET, Boodt PI, Hudson JA. Hydromechanical behaviour of joints in the Carnmenellis Granite, S.W. England. In: O. Stephansson, editor. Proceedings of the international symposium fund rock joints, Bjorkliden, Sweden, 1985. p 249–57.
[16] Raven KG, Gale JE. Water flow in a natural rock fracture as a function of stress and sample size. Int J Rock Mech Min Sci 1985;22(4):251–61.
[17] Schrauf TW, Evans DD. Laboratory studies of gas flow through a single natural fracture. Water Resourc Res 1986;22(7):1038–50.
[18] Gale JE. Comparison of coupled fracture deformation and fluid flow models with direct measurements of fracture pore structure and stress-flow porosities. In: Proceedings of 28th US symposium on rock mechanics. Tucson: Arizona; 1987. p. 1213–22.
[19] Gentier S. Comportement hydroméchanique d'une fracture naturelle sous contrainte normale. In: Proceedings of sixth congress international soceity of rock mechanics, Montreal, 1987. p. 105–8.
[20] Pyrak-Nolte LJ, Myer LR, Cook NGW, Witherspoon PA. Hydraulic and mechanical properties of natural fractures in low permeability rock. In: Proceedings of sixth congress international society on rock mechanics, montreal, 1987. p. 225–31.
[21] Sundaram PN, Watkins DJ, Ralph WE. Laboratory investigations of coupled stress-deformation-hydraulic flow in a natural rock fracture. In: Proceedings of the 28th US symposium of rock mechanics, Tucson, 1987. p. 585–92.
[22] Witherspoon PA, Wang JSY, Iwai K, Gale JE. Validity of cubic law for fluid flow in a deformable rock fracture. Water Resourc Res 1980;16(6):1016–24.
[23] Durham WB, Bonner BP. Closure and fluid flow in discrete fractures. In: Proceedings of conference fractured on jointed rock masses. California: Lake Tahoe; 1995. p. 441–6.
[24] Sun Z, Gerrad C, Stephansson O. Rock joints compliance tests for compression and shear loads. Int J Rock Mech Min Sci 1985; 22(4):197–213.
[25] Bart M, Sibai M, Shao JF. Modelling of hydromechanical behaviour of rock joints under normal stress. In: Proceedings of EUROCK 2000, Aachen, Germany, 2000. p. 591–6.
[26] Gale JE. The effects of fracture type (induced versus natural) on the stress-fracture closure-fracture permeability relationships. In: Proceedings of 23rd US symposium on rock mechanics, Berkeley, 1982. p. 290–8.
[27] Lamas LN. An experimental study of the hydromechanical properties of granite joints. In: Proceedings of eighth international congress on rock mechanics, Tokyo, 1995. p. 733–8.
[28] Iwano M, Einstein H. Laboratory experiments on geometric and hydromechanical characteristics of three different fractures in granodiorite. In: Proceedings of eighth international congress on rock mechanics, Tokyo, 1995. p. 743–50.
[29] Hopkins DL. The implications of joint deformation in analyzing the properties and behaviour of fractured rock masses, underground excavations, and faults. Int J Rock Mech Min Sci 2000;37:175–202.